



# Optimum Design of the Dental Air-Turbine Handpiece System Using the Design of Experiment Method

Makhsuda Juraeva<sup>1</sup> · Dong Joo Song<sup>1</sup> · Dong Jin Kang<sup>1</sup>

Received: 27 August 2019 / Revised: 1 December 2019 / Accepted: 10 December 2019 / Published online: 22 January 2020  
© The Author(s) 2020

## Abstract

An air-turbine and associated air supply tube was optimized as a dental air-turbine handpiece system. The system consists of an air-turbine with an impeller and a housing, and an air supply tube which supplies compressed-air to the air-turbine. The flow characteristics of the dental air-turbine handpiece system were investigated using ANSYS CFX. The study aimed to find the significant design parameters, and optimize them in terms of the maximum torque. The number of blades, the blade angle of the impeller and the gap between the impeller and the housing were chosen as the three major design parameters. The design of experiment technique was used to optimize two dental air-turbine handpiece systems: Type 1 was an air turbine alone and Type 2 was the air-turbine with an air supply tube. The optimization results showed that the gap between the impeller and the housing was not a significant parameter for Type 1. The maximum torque was lower for Type 2 than for Type 1. The optimized optimum blade number was the same for both types, but the blade angle and the gap differed between the two types. The blade angle and blade number were significant for Type 1, and all three design parameters were significant for Type 2. The performance improvement was greater for Type 2 than for Type 1. The performance of both optimized handpiece systems was reviewed in terms of the experimental measurements of noise level, rotational speed, and withdrawal force.

**Keywords** Air-turbine · Air tube · ANSYS CFX · Coupler · DOE · Optimization · Torque

## 1 Introduction

The dental air-turbine handpiece system has evolved rapidly over the years as its rotational power is useful for grinding teeth and repairing cavities. It is a vital equipment of dentistry to prevent, diagnose and treat diseases. With the increasing social demand such as cosmetic needs, oral hygiene and management, the importance and necessity of high speed air-turbine handpieces is also growing.

A dental air-turbine handpiece system consists of a head, neck, body and coupler, as shown in Fig. 1. The head consists of an impeller and housing, and the impeller rotates at a high speed by means of air flow. An air supply tube goes through the neck, body and coupler; it supplies compressed air to the head.

A major concern of the dental air-turbine handpiece system is to increase the rotational speed of the impeller, thereby increasing the operability and cutting ability [1, 2]. Some studies have improved the turbine torque by studying the flow characteristics inside the head. For example, Lee et al. [3] studied the effects of the impeller blade shape on the performance of a head by using a steady state computational model. According to their study, an increase of the reflection angle of a blade leads to an increase in the turbine torque. Hsu et al. [4] showed that the impeller blade shape and the gap between the housing and the impeller (henceforth, simplified as ‘the gap’) affect the turbine torque. Beigzadeh et al. [5] focused on the air inlet pressure, density and impeller blade. They showed that the turbine torque is linearly proportional to the inlet pressure.

Computational fluid dynamics (CFD) is also used in designing or/and optimizing a dental air-turbine handpiece system. Muller et al. [6] used CFD simulations to optimize the air turbine geometries such as the diameter of air inlet nozzle, the diameter of the air turbine, and the gap. Califano et al. [7] used a two-dimensional flow model to design a turbine head of saw tooth shape. Juraeva et al. [8] have applied

✉ Dong Jin Kang  
dj kang@yu.ac.k

<sup>1</sup> School of Mechanical Engineering, Yeungnam University,  
214-1 Dae-dong, Gyeongsan, Gyeongsangbuk-do 712-749,  
South Korea



**Fig. 1** A dental air-turbine handpiece system

the design of experiment (DOE) with Minitab to optimize a turbine head of saw tooth shape. They optimized the tip width and the angle of the saw tooth blade.

However, most previous design studies focused on a dental the head of air-turbine handpiece system without any consideration of the air supply tube. Therefore, the inlet pressure and flow characteristics into the head were not properly treated. In this paper, we propose a model with an air supply tube to handle the inlet pressure and flow characteristics properly and compare the results with the solutions obtained without the air supply tube.

The flow characteristics of the air-turbine handpiece system were simulated using ANSYS CFX software [9]. We used the DOE to generate the design parameters and to analyze the optimization processes [10]. Minitab DOE software was used to assign design parameters, create a set of experimental conditions, analyze the results, transform the effects of design parameters into graphs, and predict the optimal results that meet the quality objectives. We had selected the full factorial optimization method of Minitab for optimization. The influences of the design parameters on the air-turbine handpiece system were analyzed by using analysis of variance (ANOVA).

## 2 Computational Model of the Air-Turbine System

### 2.1 Dental Air-Turbine Handpiece System and Two Computational Models

A dental handpiece consists of head, neck, body and coupler, as shown in Fig. 1. The impeller, located inside the head, rotates as compressed air is supplied through the neck. In this study, two different computational models were simulated: Type 1 is the air turbine alone, and Type 2 is the air turbine system with an air supply tube. Figure 2 shows the two computational models used in this study. Compressed air enters the head through the Air In and leaves the head through the Air Out for Type 1, while Type 2 has its inlet at the end of the air tube, as shown in Fig. 2b. For present study, we chose a commercial dental air turbine handpiece. It is Saeyang KT-500N [11], and its dimensions are listed in Table 1. The diameters of the air inlet and air outlet are 3 mm and 4 mm, respectively. Therefore, Type 1 is a

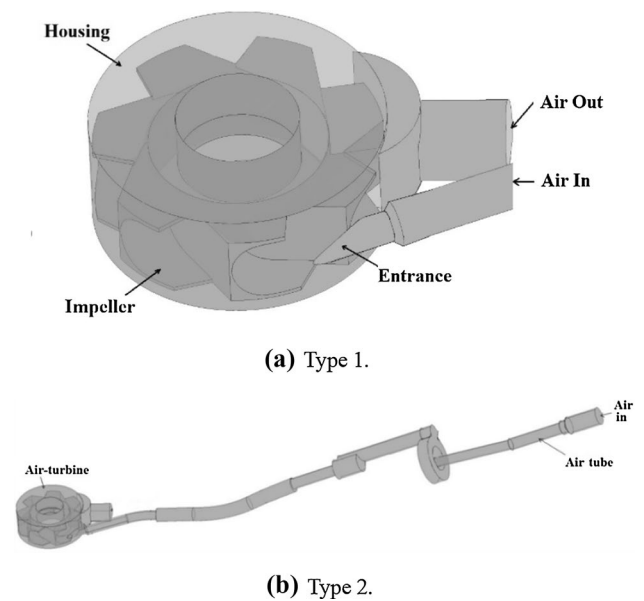


**Fig. 2** Two computational domains

simplified model of Saeyang KT-500N [11]. Type 2 extends Type 1 including an air supply tube.

### 2.2 CFD Analysis and Grid Validation

Two computational models of Types 1 and 2 were simulated to study the flow characteristics and analyze the influential design parameters. All simulations were carried out using ANSYS CFX software. The rotational motion of the impeller was treated by the immersed solid method, which is a fluid–structure interaction option of CFX. The rotational motion changes periodically the inlet pressure to the head. Therefore, all computations should be unsteady to include properly the effects of inlet pressure to the head. The Reynolds-averaged Navier–Stokes equations with the  $k$ – $\epsilon$  turbulence model [12] were used to treat the turbulent flow. As the flow field in question may not include any massively separated flow zone and the purpose of this paper is to optimize relevant design variables, the  $k$ – $\epsilon$  model was used as in the other papers [5, 7]. Additionally, we adopted

**Table 1** Dimensions of the impeller

Inner radius impeller (mm)	3.5
Outer radius of impeller (mm)	5.65
Blade angle (°)	90
Number of blades	8
Gap (mm)	0.11
Height of housing (mm)	4.75
Diameter of housing (mm)	11.41

the non-equilibrium wall function to resolve the near wall behavior of a turbulent flow [9].

Figure 3 shows a schematic of the air-turbine: A indicates the tip, B is the bucket and C is the back side of a blade. The blade angle is defined as the angle between two adjacent blades, and the rotational angle as the angle from the entrance to the center of a blade.

To check the grid independence of numerical solutions, a set of preliminary simulations was carried out for Saeyang KT-500N [11]. At the inlet, the total pressure was set at 3 bar and the outlet pressure was assumed to be equal to the atmospheric pressure. The rotational speed of the impeller was assumed to be 300,000 rpm. Table 2 summarizes the solver and boundary conditions used for the simulation. The grid system was generated with hexagons. The number of elements was varied from 1.5 million to about 4.5 million for Type 1. The same grid density was used for Type 2. The time step for the computation was  $5.6 \times 10^{-7}$  s. The computational results were obtained using parallel computers running on a Linux operating system. The wall clock time to compute a case requires about 2 days.

The handpiece system was divided into parts such as head, impeller, input and output to generate grid. The grid

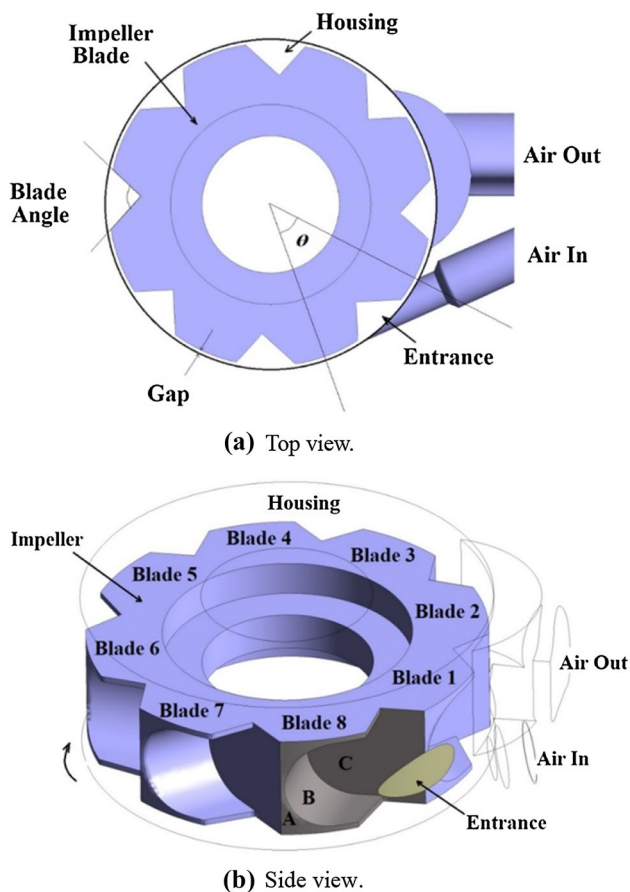
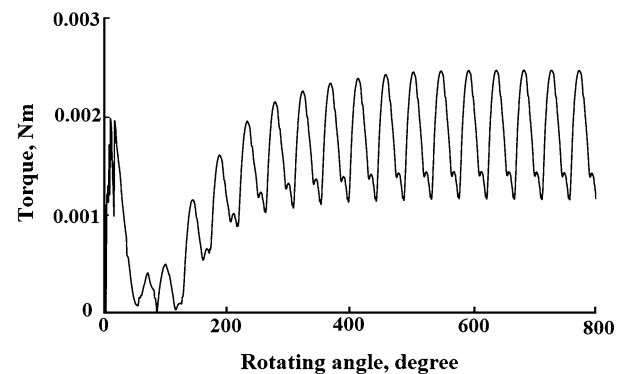


Fig. 3 Schematic of the air-turbine

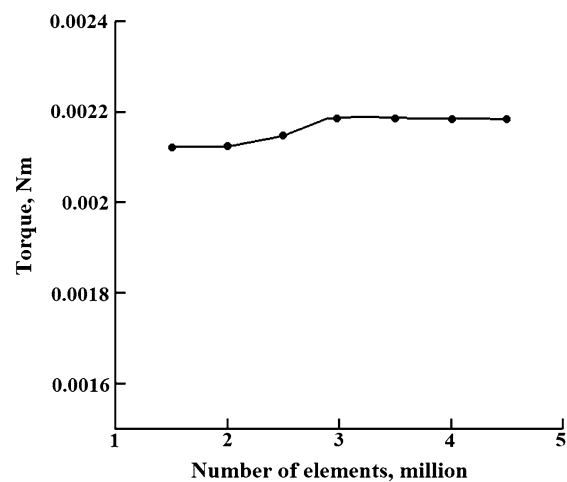
Table 2 Boundary and solver conditions for the computation

Software	CFX
Air property	Incompressible
Impeller rotation	Immersed solid method
Analysis type	Unsteady
Time step, (s)	$5.5556 \times 10^{-07}$ (1/360°)
Rotational speed, RPM	300,000
Turbulence model	k- $\epsilon$
Inlet (total pressure)	3 bar
Outlet	0 bar
Wall	No-slip

was generated separately with hexagonal grid for each part. For the grid validation, the number of elements was varied from 1.5 million to about 4.5 million for Type 1. The same grid density was used for Type 2. We used the residue of all governing equations as a convergence criterion, and set it at 0.001. We stopped the unsteady computation when the



(a) Evolution of the torque with rotating angle.



(b) Torque value with number of elements.

Fig. 4 Results of grid validation test

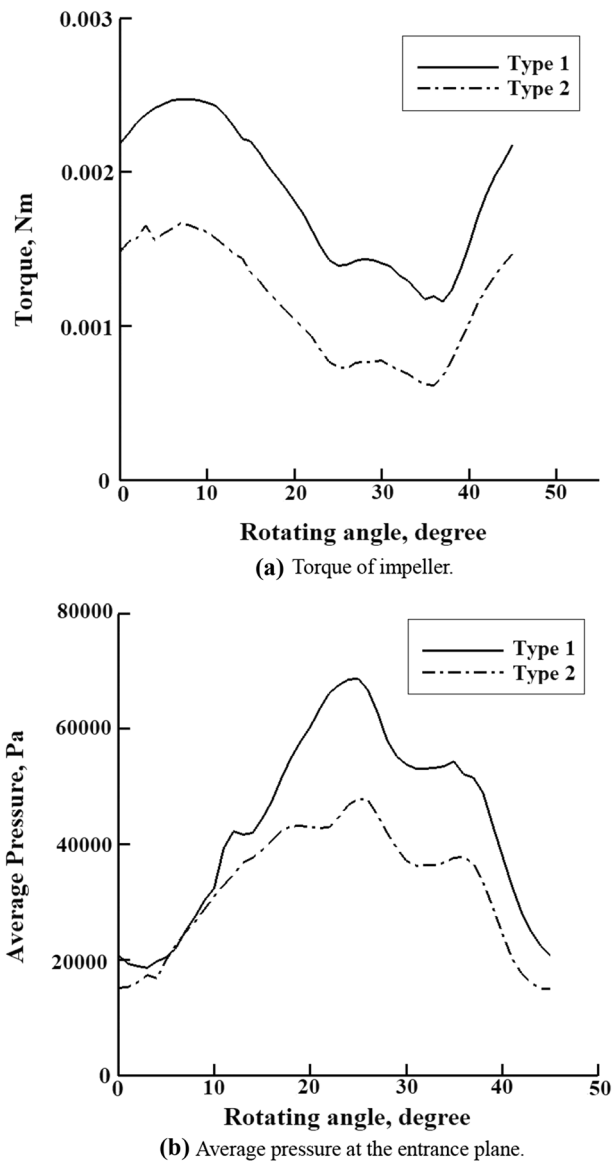


Fig. 5 Comparison of characteristics of type 1 and type 2

variation of torque between two consecutive periods is less than 0.1%.

Figure 4a shows an evolution of the torque with the rotation angle, and a periodic behavior is obtained after about  $500^\circ$ . Hereafter, the relative variation between two consecutive periods is less than 0.1%. Figure 4b shows the dependence of the maximum torque on the number of cells. The torque was calculated by computing the moment acting on the every blade. The results show that the numerical solutions obtained with more than about 3.2 million are accurate enough for the present study: its relative error is less than 0.13%. Therefore, all computations reported in this paper were simulated with an element size of less than or equal to the case of 4 million. We checked wall proximity of mesh

by calculating the dimensionless wall distance  $y^+$  along the blade, and it varied within the range of 120.

### 3 Results and Discussion

#### 3.1 Flow Characteristics of Type 1 and Type 2

A set of computations was carried out to understand how the inclusion of an air supply tube affects the flow characteristics. For the computations, the blade angle, the gap between the impeller and the housing, and blade number were set as  $90^\circ$ , 0.11 mm and 8, respectively. The rotational speed of the impeller was 300,000 rpm. Both Types 1 and 2 were simulated under the same experimental conditions.

Figure 5a compares the torque of Types 1 and 2. As the impeller has 8 blades, the rotational angle of  $45^\circ$  means the duration for the passing of one blade. Both curves show a sinusoidal distribution of torque with the rotational angle, and the maximum torque occurs at the same rotational angle of  $8^\circ$ . However, the torque of Type 1 is larger than that of Type 2. Figure 5b compares the temporal evolution of the average pressure at the entrance to the head for Types 1 and 2. The average pressure is calculated by computing the static pressure at the entrance plane shown in Fig. 3. It shows three peaks during the passing of one blade passing. The pressure peaks are observed at the rotational angles of  $12^\circ$ ,  $25^\circ$ ,  $35^\circ$  for Type 1, and of  $16^\circ$ ,  $25^\circ$ ,  $38^\circ$  for Type 2. The relative magnitude of the pressure peaks also differs between Types 1 and 2.

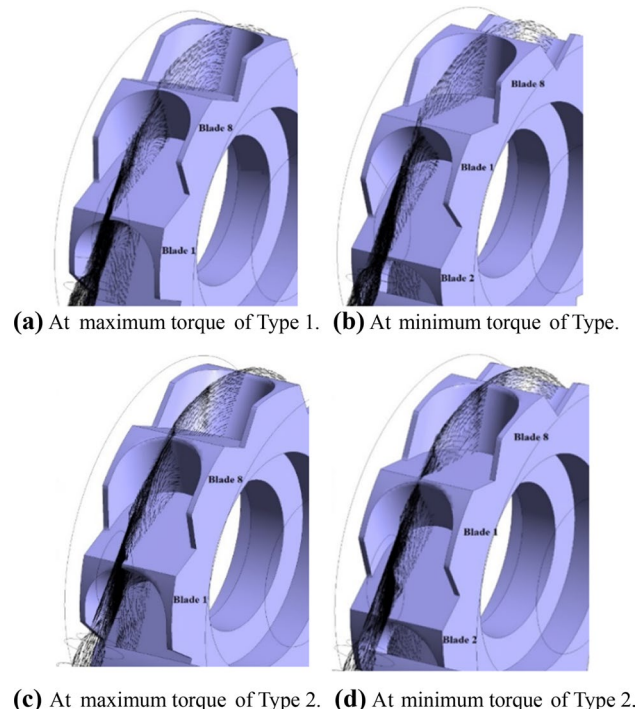


Fig. 6 Blade positions for types 1 and 2

The highest pressure peak is observed when the jet from the entrance impinges on the blade face, B in Fig. 3b, at the right angle. Consequently, the blade angle and blade number can change the torque distribution. The second and third pressure peaks are formed as the jet from the entrance impinges on the blade face at acute and obtuse angles, respectively. So, some of the jet flows through the gap between the impeller and the housing, which suggests that the gap is an important design parameter [13]. For Type 2, the pressure is reduced by about 25% along the air supply tube. A prominent difference in the flow characteristics between the two types is more obviously observed at the entrance to the impeller, as shown in Fig. 5.

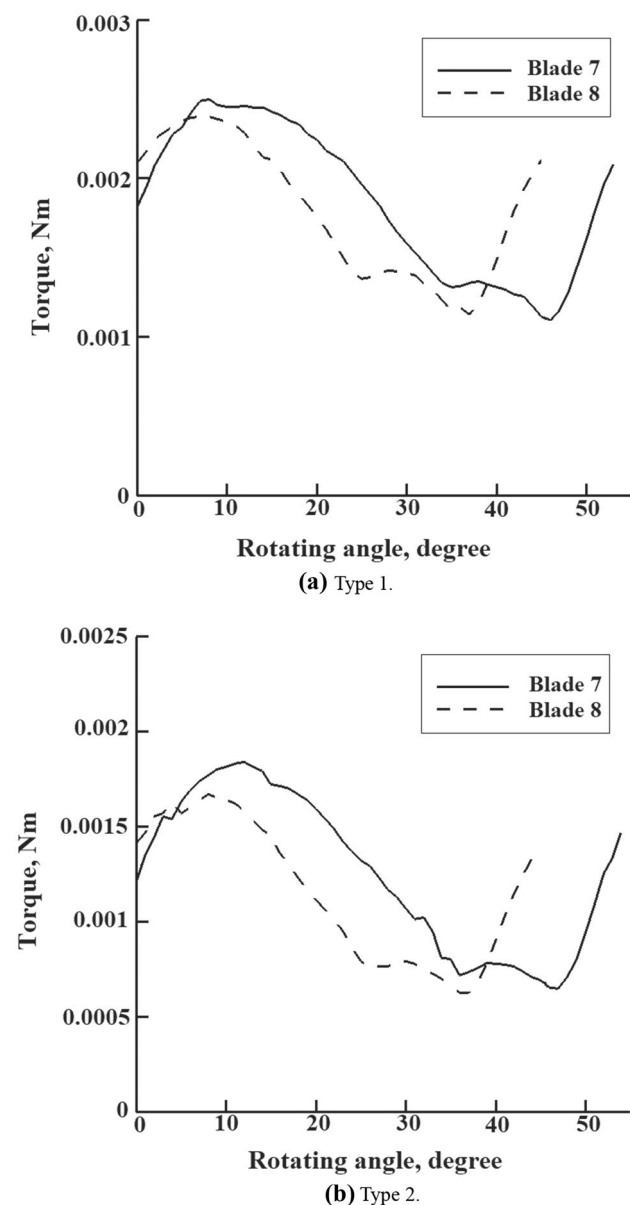


Fig. 7 Comparison of torque distributions with the blade number

Table 3 Variation of maximum torque of types 1 and 2

Type	Blade	Angle (°)	Gap (mm)	Max torque (Nm)
1	7	90	0.11	0.002647
1	8	90	0.11	0.002473
1	7	100	0.11	0.002349
1	7	90	0.15	0.002387
2	7	90	0.11	0.001893
2	8	90	0.11	0.001797
2	7	100	0.11	0.001930
2	7	90	0.15	0.001782

Figure 6 compares the flow characteristics at the blade position of the maximum and the minimum torque for Types 1 and 2. The figure shows that the blade positions are almost the same for Types 1 and 2. However, the rotational angle for the maximum torque is not coincident with the angle of the pressure peaks. The torque is the value integrated over all the blade surfaces, while the pressure is calculated at the plane entering to the impeller. Therefore, the rotational angle is not necessarily coincident with the angle of the pressure peaks. The maximum torque is determined by a combination of all the design factors and the inlet pressure to the head.

### 3.2 The Design Parameters of the Air-Turbine Handpiece System

Among the various geometric parameters of the air turbine, the blade number, blade angle and gap were chosen as the three major parameters based on the results of previous studies [8].

Figure 7 shows how the blade number affects the torque for Types 1 and 2. The torque distributions according to rotational angle of the impeller were obtained during the rotational angle of the passing of one blade the entrance. All of the torque distributions show similar behavior, but their relative magnitude is clearly dependent on the blade number.

Table 3 presents the maximum torque of both types for several values of the design variables. The results show that the maximum torque is greatly affected by all three design parameters. Therefore, we can use the maximum torque as an object function to optimize the design parameters.

Table 4 Design parameters of the air-turbine

	6	7	8
Number of blades	6	7	8
Blade angle (°)	80	90	100
Gap (mm)	0.11	0.13	0.15



**Fig. 8** Interaction and main effects of the three design parameters of ▶ type 1 and type 2

### 3.3 Optimization of The Air-Turbine Handpiece System Using DOE and Experimental Validations

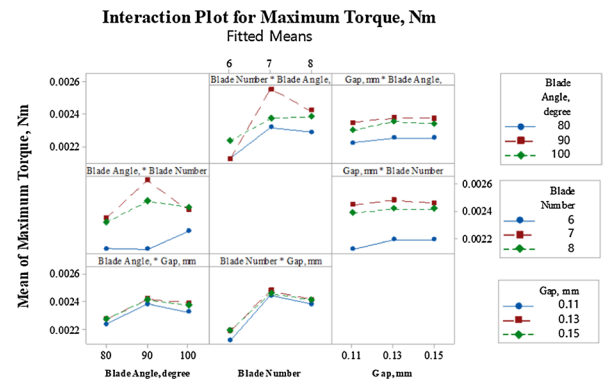
A factorial method was used to study the influence of the three design parameters for Types 1 and 2. According to the results, the gap, blade angle and blade number are influential design parameters for both types. The maximum torque was chosen as the object function.

The optimization of each design parameter was investigated for three parameter values that cover the range of values typically found in commercial applications [11]. The number of blades was varied from 6 to 8. The blade angle was varied from 80° to 100°, and the gap was from 0.11 to 0.15 mm. Therefore, the total number of simulations is 27. We used the factorial design method to maximize the torque by combining the design parameters. Table 4 summarizes all possible configurations of the three design parameters. The factorial design method was used to maximize the torque by combining the design parameters.

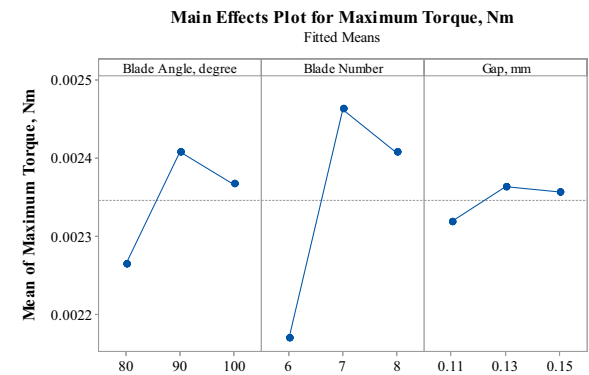
Figure 8 shows the interaction and main effects of the design parameters of Type 1 and Type 2 on the maximum torque. Here, the interaction effects represent the combined effects of arbitrary two design parameters, and the main effect is the effect of each design parameter. The mean of maximum torque is the average of the maximum torques obtained for all possible values of the other design parameter. For example, the mean of maximum torque for the interaction effects of the blade angle and the gap is calculated by averaging all the maximum torques obtained for the number of blades 7, 8, and 9. For Type 1, Fig. 8a, b show that the gap has little effect on the maximum torque, and it is not coincident with the previous study [5]. This result suggests that Type 1 is not a suitable model to deal with the effects of gap. On the contrary, Fig. 8c, d show that all the three design parameters play meaningful roles in the interaction and main effects for Type 2. The significance of each design parameter is checked in detail using ANOVA, and the result is described below.

The optimization results for Types 1 and 2 are summarized in Table 5. The composite desirability is 0.9610. Here, the composite desirability (D) evaluates how the design parameters optimize the turbine torque overall. The desirability has a range of zero to one. One represents the ideal case, and zero indicates that the optimization is outside the acceptable limits of design parameters [10]. Among the three design parameters, the gap is the most affected by the presence or absence of the air supply tube, which suggests that the gap is crucial for optimizing the flow characteristics entering into the head.

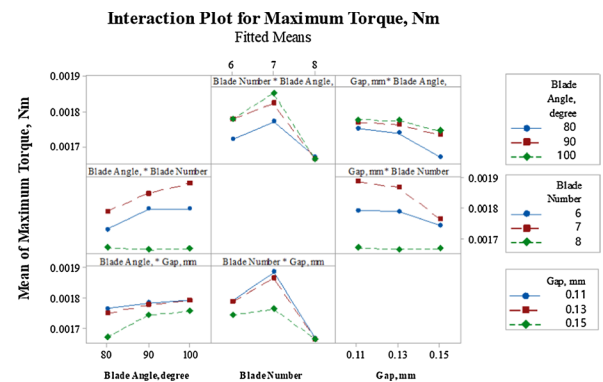
The optimized maximum torque of Type 1 is 0.00266 Nm with 7 blades, a blade angle of 90° and a gap of 0.13 mm.



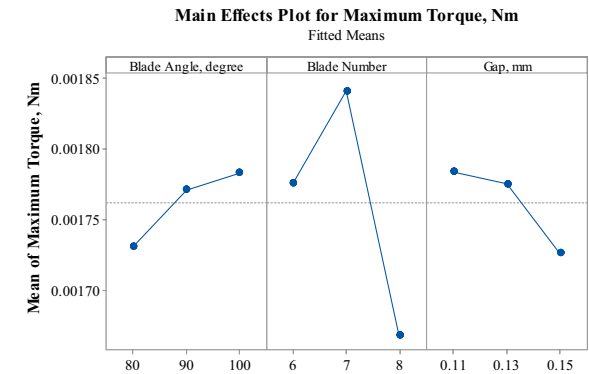
(a) Interaction effects of design parameters for Type 1.



(b) Main effects of design parameters for Type 1.



(c) Interaction effects of design parameters for Type 2.



(d) Main effects of design parameters for Type 2.

**Table 5** Optimized design parameters for type 1 and 2

	Blade number	Blade angle (°)	Gap (mm)	Torque (Nm)
Type1	7	90	0.13	0.0026
Type2	7	100	0.11	0.00193
Type1	Significant	Significant	Not significant	
Type2	Significant	Significant	Significant	

On the other hand, the optimized maximum torque of Type 2 is 0.00193 Nm. The optimization result of Type 2 is with 7 blades, a blade angle of 100° and a gap of 0.11 mm.

The optimization results were analyzed further using ANOVA. For Type 1, the blade angle and number of blades were statistically significant ( $p < 0.05$ ), while the gap was insignificant ( $p = 0.075$ ). For Type 2, all three design parameters were statistically significant ( $p < 0.05$ ). Here, the  $p$  value is defined as the probability for the variate to be observed as a value equal to or more extreme than the value observed. Therefore, the smaller the  $p$  value, the higher the significance in ANOVA. If the  $p$  value is less than a specified significance level (usually 0.05), we declare the result to be statistically significant [10].

Korea textile machinery institute (KOTMI) evaluated the performance of the three turbine systems: two optimized handpiece turbine systems and Saeyang KT-500 N [14]. All measurements were made at 20 °C room temperature, 1 bar atmospheric pressure and 40% R.H. The inlet pressure was set at 3 bar. KOTMI measured the performance in terms of noise level, rotational speed, and withdrawal force. The withdrawal force is widely used to estimate the cutting power of a dental handpiece turbine system [15]. As the optimization is performed in the viewpoint of the fluid dynamics, the effects of optimization are reflected in these three parameters. We quote their results as a kind of experimental validation.

Table 6 presents the experimental results of both the optimized turbine systems and Saeyang KT-500 N. Both optimized models of Type 1 and Type 2 show noticeable improvement from Saeyang KT-500 N in terms of the rotational speed and withdrawal force. As the rotation of the head is powered by the fluid flow, a faster rotation suggests that the friction resistance due to the fluid flow is small. The maximum torque of a handpiece turbine is proportional to

the withdrawal force. Therefore, a handpiece turbine system having larger withdrawal force means a more powerful system. As the rotational speed increases, the noise level is also increase in general. However, the increase of the noise level of Type 2 from that of Saeyang KT-500 N is quite limited. Therefore, Type 2 shows the best performance among the three cases listed in Table 6. In summary, the experimental results support qualitatively that Type 2 performs better than Type 1 in optimizing the design parameters of a dental handpiece turbine system.

## 4 Conclusions

Two computational domains for the optimization of an air-turbine handpiece system were investigated using CFD and DOE: Type 1 is an air turbine alone and Type 2 consists of an air-turbine with a corresponding air supply tube. The flow characteristics of the air-turbine handpiece system were simulated using ANSYS CFX software. The design parameters were optimized using the DOE method of Minitab software. The blade angle, blade number and gap between the housing and the impeller were selected as the three design parameters, and the numerical simulation results were reviewed by an experimentation.

The optimization of each design parameter was investigated for three parameter values that cover the range of values typically found in practical applications. The blade number was 6, 7 and 8, the blade angle was 80°, 90° and 100°, and the gap was 0.11, 0.13 and 0.15 mm. The maximum torque was optimized at the blade angle, blade number and gap of 90°, 7, and 0.13 mm for Type 1 and of 100°, 7, and 0.11 mm for Type 2, respectively. The optimized values differed between the two types due to differences in the flow characteristics at the entrance to the head.

All three design parameters were significant for the optimization of Type 2, but for the optimization of Type 1 only the blade angle and blade number were significant, whereas the gap was insignificant. Type 2 is therefore a more suitable model to include the effects of the inlet pressure in the optimization of an air-turbine handpiece system.

The experimental comparison of the optimized designs with Saeyang KT-500 N in terms of noise level, rotational speed, and withdrawal force suggests that the performance of the dental handpiece turbine can be improved by the optimization using

**Table 6** Comparison of the experimental results

	Saeyang KT-500N	Optimized type 1	Optimized type 2
Noise (dBA)	69.1	79.2	70.6
Rotational speed (rpm)	277,680	284,520	333,780
Withdrawal force (N)	22.1	24.3	26

either Types 1 or 2. Especially, Type 2 showed an additional performance improvement compared with that of Type 1.

**Acknowledgements** This study was conducted with the support of the Ministry of Trade, Industry and Energy, Specialized Local Industry Development Project (R&D) of Korea Institute for Advancement of Technology.

**Funding** Funding was provided by Korea Institute for Advancement of Technology (Grant No. R0003688).

**Open Access** This article is licensed under a Creative Commons Attribution 4.0 International License, which permits use, sharing, adaptation, distribution and reproduction in any medium or format, as long as you give appropriate credit to the original author(s) and the source, provide a link to the Creative Commons licence, and indicate if changes were made. The images or other third party material in this article are included in the article's Creative Commons licence, unless indicated otherwise in a credit line to the material. If material is not included in the article's Creative Commons licence and your intended use is not permitted by statutory regulation or exceeds the permitted use, you will need to obtain permission directly from the copyright holder. To view a copy of this licence, visit <http://creativecommons.org/licenses/by/4.0/>.

## References

- Dyson, J. E., & Darvell, B. W. (1999). Flow and free running speed characterization of dental air-turbine handpieces. *Journal of Dentistry*, 27, 465–477.
- Dyson, J. E., & Darvell, B. W. (1999). Torque, power and efficiency characterization of dental air-turbine handpieces. *Journal of Dentistry*, 27, 573–586.
- Lee, J. H., & Kim, K. S. (2009). Numerical study on the effect of turbine blade shape on performance characteristics of a dental Air turbine handpiece. *Korean Society of Machine Tool Engineers*, 13, 34–42. (in Korean).
- Hsu, C. N., Chiang, H. W., & Chang, Y. Y. (2011). Numerical simulation and experimental study of a dental handpiece air turbine. *International Journal of Turbo and Jet Engines*, 28(2), 159–168.
- Beigzadeh, B., Derakhshan, S., & Zia Shamami, D. (2017). A numerical study on performance of dental air turbine handpieces. *Mechanika*, 23(5), 750–755.
- Müller, C., Reichenbach, U. G., & Aurich, J. C. (2014). Design and numerical simulation of an air turbine for a high frequency tool spindle. In *ICOMM*, N30.
- Califano, G., Notarib, A., Scorza, S., & Tommasi, M. (2016). “Design and CFD analysis of an odontoiatric turbine. In *Proceedings of ECOS 2016*.
- Juraeva, M., Ryu, K. J., & Song, D. J. (2014). Optimum design of a saw-tooth-shaped dental air-turbine using design of experiment. *International Journal of Precision Engineering and Manufacturing*, 15(2), 227–234.
- Ansys, C. F. X. (2009). *ANSYS Workbench, ICFM-CFD, CFX Pre. CFX-Solver: CFX-Post User's Manual*.
- Minitab Inc. (2010) *MINITAB 16: Minitab 16 User guide*.
- Saeyang. (2017). Development of ultra-high speed air turbine optic, non-optic handpiece for dental treatment. *Final report*. [www.saeyang.com](http://www.saeyang.com).
- Menter, F. R. (1994). Two-equation eddy-viscosity turbulence models for engineering applications. *AIAA-Journal*, 32, 269–289.
- Seto, W. C. (2004). *Design factors affecting air turbine handpiece performance*. Hong Kong: University of Hong Kong. [https://doi.org/10.5353/th\\_b3195438](https://doi.org/10.5353/th_b3195438).
- KOTMI (2017). The capacity evaluation of dental high-speed air-turbine. *Final report*. <https://www.kotmi.re.kr/>.
- Sirona Dental Systems GmbH. (2012). T4 high speed handpiece. *Sirona Technical Documentation*. <https://manuals.serona.com/>.

**Publisher's Note** Springer Nature remains neutral with regard to jurisdictional claims in published maps and institutional affiliations.



**Makhuda Juraeva** received her B.E degree in Applied Mathematics and Mechanics from Uzbekistan National University. She received her M.E and Ph.D. degrees in Mechanical Engineering from Yeungnam University, Gyeongsan, Korea 2003 and 2007, respectively. She is currently foreign researcher at the School of Mechanical Engineering of Yeungnam University. Her research interests include fluid flow simulation and optimization.



**Dong Joo Song** is currently a Professor at the School of Mechanical Engineering, Yeungnam University, Korea. Prof. Song's research interests include CFD, thermo-fluids system design, optimization, plastic injection molding, and thermophysics.



**Dong Jin Kang** received his M.E. and Ph.D degree in Mechanical Engineering from KAIST, Seoul, Korea in 1987 and 1991, respectively. He is currently Professor at the School of Mechanical Engineering of Yeungnam University, Gyeongsan, Korea. His research interests include optimization and simulations of fluid flow and heat transfer in machinery and micro devices.